AMERICAN SOCIETY FOR MICROBIOLOGY | Journal of Virology

Heparan Sulfate Binding Promotes Accumulation of Intravitreally Delivered Adeno-associated Viral Vectors at the Retina for Enhanced Transduction but Weakly Influences Tropism

Kenton T. Woodard,[a,b] Katharine J. Liang,[a,b] William C. Bennett,[b] R. Jude Samulski[b,c]

Neurobiology Curriculum, University of North Carolina, Chapel Hill, North Carolina, USA[a]; Gene Therapy Center, University of North Carolina, Chapel Hill, North Carolina, USA[b]; Department of Pharmacology, University of North Carolina, Chapel Hill, North Carolina, USA[c]

ABSTRACT

Many adeno-associated virus (AAV) serotypes efficiently transduce the retina when delivered to the subretinal space but show limited success when delivered to the vitreous due to the inner limiting membrane (ILM). Subretinal delivery of AAV serotype 2 (AAV2) and its heparan sulfate (HS)-binding-deficient capsid led to similar expression, indicating transduction of the outer retina occurred by HS-independent mechanisms. However, intravitreal delivery of HS-ablated recombinant AAV2 (rAAV2) led to a 300-fold decrease in transduction compared to AAV2. Fluorescence *in situ* hybridization of AAV transgenes was used to identify differences in retinal trafficking and revealed that HS binding was responsible for AAV2 accumulation at the ILM. This mechanism was tested on human *ex vivo* retinas and showed similar accumulation with HS-binding AAV2 capsid only. To evaluate if HS binding could be applied to other AAV serotypes to enhance their transduction, AAV1 and AAV8 were modified to bind HS with a single-amino-acid mutation and tested in mice. Both HS-binding mutants of AAV1 and AAV8 had higher intravitreal transduction than their non-HS-binding parent capsid due to increased retinal accumulation. To understand the influence that HS binding has on tropism, chimeric AAV2 capsids with dual-glycan usage were tested intravitreally in mice. Compared to HS binding alone, these chimeric capsids displayed enhanced transduction that was correlated with a change in tropism. Taken together, these data indicate that HS binding serves to sequester AAV capsids from the vitreous to the ILM but does not influence retinal tropism. The enhanced retinal transduction of HS-binding capsids provides a rational design strategy for engineering capsids for intravitreal delivery.

IMPORTANCE

Adeno-associated virus (AAV) has become the vector of choice for viral gene transfer and has shown great promise in clinical trials. The need for development of an easy, less invasive injection route for ocular gene therapy is met by intravitreal delivery, but delivery of AAV by this route results in poor transduction outcomes. The inner limiting membrane (ILM) creates a barrier separating the vitreous and the retina. Binding of AAV to heparan sulfate proteoglycan (HSPG) at the ILM may allow the virus to traverse this barrier for better retinal transduction. We show that HSPG binding is correlated with greater accumulation and penetration of AAV in the retina. We demonstrated that this accumulation is conserved across mouse and human retinas and that the addition of HSPG binding to other AAV capsids can increase the number of vectors accumulating at the ILM without dictating tropism.

Adeno-associated virus (AAV) is a small (25-nm), nonpathogenic virus that has been extensively studied as a vector for gene transfer applications (1–3). The virus consists of two parts: the viral genome and the protein capsid. The viral genome can be largely replaced with a desired transgene to create recombinant AAV (rAAV) vectors used for gene delivery. The protein capsid is responsible for cell attachment and entry via a variety of glycans and cell surface receptors. There are 11 naturally occurring serotypes of AAV, denoted AAV1 to AAV11. Glycans and receptors have been elucidated for several AAV serotypes. Heparan sulfate proteoglycan (HSPG) has been shown to be used for both rAAV2 and rAAV3 cell entry (4). rAAV6 displays dual-glycan interaction with HSPG and sialic acid; however, HSPG binding alone is insufficient for cellular entry (5). Various linkages of sialic acid are important for the transduction of the rAAV1, rAAV4, and rAAV5 serotypes (6, 7). N-linked galactose is used for the transduction of the rAAV9 serotype (8). Glycans expressed on the cell surface dictate the tissue and cellular tropism observed with the various AAV capsids. In addition to attachment to these glycans, AAV serotypes interact with cell receptors, including human growth factor receptor, integrins, and laminin receptors (9–11).

rAAV has shown promise for retinal gene transfer (12–16). In addition to the influence of the capsid discussed above, the route of administration to the retina determines the transgene expression profile and efficacy. Subretinal (SR) delivery deposits the vec-

Received 8 August 2016 **Accepted** 15 August 2016

Accepted manuscript posted online 24 August 2016

Citation Woodard KT, Liang KJ, Bennett WC, Samulski RJ. 2016. Heparan sulfate binding promotes accumulation of intravitreally delivered adeno-associated viral vectors at the retina for enhanced transduction but weakly influences tropism. J Virol 90:9878–9888. doi:10.1128/JVI.01568-16.

Editor: R. M. Sandri-Goldin, University of California, Irvine

Address correspondence to R. Jude Samulski, rjs@med.unc.edu.

Supplemental material for this article may be found at http://dx.doi.org/10.1128/JVI.01568-16.

tor between the outer nuclear layer (ONL) and the retinal pigment epithelium (RPE), which causes detachment of these two layers to accommodate the injected solution. Many AAV serotypes display transduction in the ONL and RPE layers, with some serotypes showing restricted tropism (16). Of the natural serotypes, rAAV8 is one of the best for SR delivery based on its rapid transgene expression and transduction of all retinal layers (17, 18). In addition to SR delivery, vectors can be administered to the vitreous. Intravitreal (IVit) delivery of rAAV vectors has become the preferred route to the SR space for several reasons, including (i) technical ease of injection, (ii) the potential to deliver vector to a greater area of the retina, and (iii) less damage to the retina. For clinical applications, IVit delivery can be performed as an outpatient procedure and would not exclude patients with severe retinal degeneration. However, few serotypes exhibit efficient transduction by this route (19). rAAV2 is one of the few serotypes tested in multiple animal models, typically resulting in the transduction of retinal ganglion cells (RGC) (19–22). In rodent models, transduction with this serotype has been seen in occasional Müller glia, amacrine, and horizontal cells. In addition, rAAV6 expression in the RGC and inner nuclear layer (INL) has been seen in rodent models (23–25). Understanding viral trafficking and barriers to efficient IVit transduction provides opportunities to rationally design capsids to overcome current limitations.

At the vitreoretinal junction, the inner limiting membrane (ILM) has been implicated as the barrier responsible for the inefficiency of most rAAV vectors in transducing the retina. Despite the limited transduction, several AAV serotypes are capable of accumulating at the vitreoretinal junction following delivery (19, 20). Injections of fluorescently labeled capsids (rAAV1, -2, -5, -8, and -9) into the vitreous of adult rodents showed that rAAV2, rAAV8, and rAAV9 accumulated at the ILM, but only rAAV2 resulted in transduction (19). With a degenerated ILM, all of these AAV serotypes were capable of transducing the retina (20). The ILM is composed of the extracellular matrix of the Müller glial endfeet, which display an array of glycans similar to those of other basement membranes (26, 27) and prevent access to cells needed for AAV transduction. The binding of rAAV2, rAAV8, and rAAV9 is likely explained by laminin interaction; however, accumulation of laminin appears insufficient for transduction of rAAV8 and rAAV9. HSPG binding of rAAV2 could explain the selective transduction, but enzymatic digestion of HSPG has been shown to increase the transduction and penetration of rAAV2 in the retina (28). Because rAAV2 has shown HSPG-independent transduction in other tissue (29, 30), it is possible that rAAV2 does not need HSPG binding for retinal transduction and that HSPG may prevent the spread of rAAV2 particles to the outer retina. Thus, rAAV2 capsid interactions with HSPG at the ILM compose the rate-limiting step for efficient IVit transduction of the retina. Understanding these interactions will help guide the rational design of vectors for more efficient IVit transduction.

To study rAAV interactions at the ILM, we used a collection of capsids with altered glycan usage. We used a self-complementary chicken β-actin, shortened form (CBh)–green fluorescent protein (GFP) cassette for optimized transgene performance. The CBh promoter is a shortened form of the chicken β-actin (CBA) promoter with the addition of cytomegalovirus (CMV) enhancer elements. The CBh promoter has shown exceptional activity in other neuronal tissue compared to CMV or CBA promoter activity (31) without potential silencing issues, and its small size is beneficial for maximizing the limited transgene capacity of rAAV. The self-complementary form of the transgene facilitates faster expression that is more robust than that of the classic single-stranded form (17, 32, 33). This self-complementary form can also facilitate production of transgene product in cells that do not provide second-strand synthesis. In addition to optimizing GFP production, we used fluorescence *in situ* hybridization (FISH) to track the vector following IVit delivery to obtain an accurate picture of rAAV trafficking. Genetic capsid mutations were used to understand the role of heparan sulfate (HS) binding in rAAV transduction of the mouse retina without modifying the ILM structure. We used known capsid mutations in the HS-binding footprint of rAAV2 to carry out this analysis. The motif on the rAAV2 capsid consists of a basic patch of residues (R484, R487, K532, R585, and R588) at the base of the 3-fold spike (30). Capsid mutants, like rAAV2i8, replace residues 585Q and 588T to ablate HS binding and alter tropism away from HS-rich liver tissue to become more systemic when delivered intravenously (29). Using these capsid mutants, we investigated the unilateral necessity for HS binding in retinal transduction.

MATERIALS AND METHODS

Vector production and purification. Self-complementary rAAV carrying the GFP gene under the control of the ubiquitous CBh promoter (34) were produced by the triple-transfection method using polyethylenimine (35). Viruses were harvested as previously described (36). Lysate was clarified by centrifugation at 6,200 × *g* and purified by iodixanol gradient ultracentrifugation at 402,000 × *g* for 1 h. Viruses were pulled from the 40% to 60% interface, purified by ion-exchange chromatography on a 1-ml Q HyperD F column (Pall), and eluted with 200 mM NaCl, 25 mM Tris (pH 9.0). It was difficult to produce a significant yield of AAV8-E533K vector with iodixanol. Therefore, AAV8 and AAV8-E533K were purified with CsCl and then with sucrose to obtain pure vector. The viruses were dialyzed against 350 mM NaCl, 5% sorbitol in 1× phosphate-buffered saline (PBS) before being aliquoted and frozen at −80°C. The viral titer was determined by quantitative PCR (qPCR) against wild-type inverted terminal repeats (ITR) of DNase-resistant vector genomes relative to a virus standard (data not shown). The viruses underwent electrophoresis on a 1% Bis-Tris gel (Novex) with silver staining (Life Technologies) to assess purity (data not shown).

Animal injections. Adult C57BL/6 mice were used for this study. All the animals were housed under a 12-h/12-h light/dark cycle in the University of North Carolina Division of Laboratory Animal Medicine facilities and were handled in accordance within the guidelines of the Institutional Animal Care and Use Committee at the University of North Carolina. Prior to vector delivery, the animals were anesthetized with ketamine (75 mg/kg of body weight), xylazine (10 mg/kg), or acepromazine (1.5 mg/kg), and dilated with 1% tropicamide and 2.5% phenylephrine. Proparacaine-HCl was applied to the eyes as a local anesthetic. Intraocular needles were constructed using a 32G canula connected to a Hamilton syringe via tubing filled with water. An air bubble separated the water from the viral suspension. Freshly thawed viruses were diluted to working stock and incubated in the intraocular needle at room temperature for 10 min prior to injection. The needles were evacuated and loaded with fresh suspension. The viral suspension was mixed with fluorescein sodium salt (Sigma) to confirm successful injection as previously described (37). All injections were carried out by the same surgeon. For IVit injections, a pilot hole was made with the tip of a beveled 30G needle in the superior portion of the eye approximately 0.5 mm posterior to the limbus. The intraocular needle was inserted through this hole into the vitreous under direct observation through a microscope. A volume of 1 μl was delivered at a constant rate over 30 s using a syringe pump. The needle was held in place for 20 s to allow intraocular pressure equilibration before removal. For SR injection, the intraocular needle was inserted tangential

to the eye. Delivery of fluid was immediate and was characterized for success by optical coherence tomography (OCT) and fundoscopy of fluorescein distribution using the Micron IV (Phoenix Research Laboratories). Genteal (Novartis) was applied to the eyes to prevent corneal drying, and the mice were allowed to recover on heating pads.

***In vivo* imaging.** Fundus images and OCT were carried out by dilating and sedating the animals as described above. All fluorescent images were taken under the same settings and with similar retinal positions using the Micron IV. The green channel of the fluorescent fundus image was isolated, converted to grayscale, and quantified by integrated density measurements using ImageJ (National Institutes of Health).

Enucleation and histology. The animals were sedated and perfused with PBS containing 1 unit heparin per ml, followed by 4% paraformaldehyde (PFA) in PBS. The eyes were enucleated, and a puncture was made anterior to the limbus using an 18G needle before incubation in 4% PFA for 10 min. The anterior segment, musculature, and lens were removed, and eyecups were placed in 10% sucrose at 4°C overnight, followed by 20% and 30% sucrose incubations. The eyecups were embedded in OCT cutting medium (Sakura), frozen at −20°C, and stored at −80°C. Ten-micrometer transverse sections were collected on precleaned Superfrost Plus slides (Fisher) and stored at −80°C until further processing.

Immunohistochemistry (IHC) and analysis. Sections were washed in Tris-buffered saline (TBS) containing 0.3% Tween 20 (TBS-T) and incubated in blocking buffer (10% normal goat serum [NGS], 0.1% Triton X-100 in PBS) for 1 h in a humid chamber. The slides were incubated in antibody solution (3% NGS, 0.1% Triton X-100 in PBS) with primary antibodies in a humid chamber overnight at room temperature. The primary antibodies used were rabbit anti-GFP (1:500; Millipore), mouse anti-glutamine synthetase (1:100; Abcam), mouse anti-heparan sulfate 10E4 epitope (1:70; Amsbio), mouse anti-rhodopsin (1:100; Rockland), mouse anti-protein kinase C (PKC) alpha (H-7; 1:250; Santa Cruz), and fluorescein *Erythrina cristagalli* lectin (1:100; Vector Laboratories). After three washes with TBS-T, secondary fluorescent antibodies were applied in antibody solution for 2 h in a humid chamber. The secondary antibodies were Alexa Fluor 488 goat anti-rabbit (1:1,000; Molecular Probes), Alexa Fluor 568 goat anti-mouse (1:1,000; Molecular Probes), and Alexa Fluor 568 rabbit anti-goat (1:1,000; Molecular Probes). The slides were mounted in Prolong Gold antifade reagent with 4′,6-diamidino-2-phenylindole (DAPI) (Molecular Probes) according to the manufacturer's protocol. Images were taken on a LeicaSP2 AOBS upright laser scanning confocal microscope or an Olympus IX83 fluorescence microscope.

Soluble HS analog assays. For *in vitro* studies, HEK293 cells were plated in a 24-well dish at a density of 10^5 cells per well and allowed to adhere overnight at 37°C, 5% CO_2. Viruses were preincubated with soluble heparin at the specified concentrations for 1 h prior to addition to cells at a concentration of 10,000 viral genomes (vg) per cell. The cells were harvested 48 h later and quantified by flow cytometry.

Fluorescence *in situ* hybridization. The GFP gene was cloned into the pSPT18 vector (Roche RNA *in vitro* transcription kit) at the HindIII and EcoRI sites and sequenced for confirmation. Plasmids were linearized with these restriction enzymes and purified by phenol-chloroform extraction/ethanol precipitation and resuspended in water. The linearized plasmids were quantified by spectrophotometry and verified by DNA sequencing before *in vitro* transcription of antisense and sense riboprobes was carried out as described by the manufacturer (Roche). Aliquots of riboprobes were frozen in water and were quantified as described by the manufacturer and analyzed by gel electrophoresis and SYBR Gold staining (Invitrogen). Riboprobe functionality was assayed for sensitivity and selectivity by dot blotting of virus controls to a positively charged nitrocellulose membrane (Roche). The sense and antisense probes were equally able to detect the viral GFP transgene (data not shown).

Frozen slides were heated to 55°C for 10 min and pretreated as previously described (38). The slides were then incubated in hybridization buffer (50% formamide, 10 mM Tris [pH 7.6], 200 μg/ml *Saccharomyces cerevisiae* tRNA, 1× Denhardt's solution, 10% dextran sulfate, 600 mM NaCl, 0.25% SDS, 1 mM EDTA [pH 8]) without probe at a hybridization temperature of 65°C for 2 to 4 h. The slides were transferred to prehybridization buffer containing 50 ng/ml of sense riboprobe to specifically detect DNA and not mRNA transcripts. The slides were heated to 80°C for 20 min, snap chilled on ice, and incubated overnight at 65°C. The slides were washed in 50% formamide-2× SSC (1× SSC is 0.15 M NaCl plus 0.015 M sodium citrate) at 65°C for 30 min and in 2× SSC at 55°C for 20 min, with two washes with 0.2× SSC at 55°C for 20 min each time. The slides were washed in 1× washing buffer (Roche), followed by incubation with 10% sheep serum in 1× blocking buffer for 1 h in a humid chamber. Sheep anti-digoxigenin (DIG)-allophycocyanin (AP) antibody (1:1,000; Roche) was applied and incubated for 2 to 3 h in a humid chamber. The slides were washed three times in washing buffer with gentle agitation for 10 min each time, followed by two incubations in detection buffer (100 mM Tris, 100 mM NaCl, 10 mM $MgCl_2$ [pH 8.0]) for 10 min each time. HNPP/Fast Red detection substrate was prepared and applied as directed by the manufacturer (Roche) for two or three applications. Following the detection reaction, the slides were rinsed in distilled water and coverslipped using Prolong Gold antifade reagent with DAPI. Images were taken on a LeicaSP2 AOBS upright laser scanning confocal microscope or an Olympus IX83 fluorescence microscope.

***Ex vivo* human retinal-binding assay.** Human whole globes were procured immediately after death and placed in a moist chamber on ice for 4 days. The anterior chamber, iris, and lens were removed, and the globe was quartered, with some vitreous remaining attached to the retina. Ten microliters of vector was applied to the vitreous at a titer of 2×10^9 vg/μl and allowed to bind to the retina for 2 h at 4°C. The quartered retinas were kept out of medium to prevent the dispersion of the vector solution. Following the incubation, PBS was washed over the tissue, collected, and stored at −80°C. Vitreous, retina, choroid, and sclera were collected separately and stored at −80°C. The tissue samples were digested and purified using the DNeasy blood and tissue kit (Qiagen). Virus in the collected samples was quantified by qPCR using primers against the GFP and human glyceraldehyde-3-phosphate dehydrogenase (hGAPDH) housekeeping genes.

RESULTS

HS binding on rAAV2 is not required for SR transduction. A variety of AAV serotypes, both HS binding and non-HS binding, work effectively in retinal transduction when delivered subretinally, suggesting that HS binding is not needed for outer retinal transduction. To determine if rAAV2 requires HS binding in the transduction of the outer retina, HS binding was ablated using the rAAV2i8 capsid and subretinally delivered. Transductions between rAAV2 and rAAV2i8 were similar by fundoscopy. The strongest signal of GFP fluorescence could be seen within the detached area (Fig. 1a, dashed lines), but additional expression could be seen outside the bleb area for both vectors (Fig. 1a). The transduction that was outside the detachment appeared to be mostly RPE. Within the detachment, transduction of multiple layers was observed, as evidenced by the fluorescent RGC axons leading to the optic head from the site of injection (Fig. 1a, arrowhead).

IHC was used to evaluate the cell tropism between the two vectors. The RPE and ONL were the major cell layers transduced by both vectors (Fig. 1b). Areas where high RPE transduction but low ONL transduction occurred could be seen, indicating that RPE may be the predominant cell type to be transduced. Transduction of the ONL occurred predominantly in rods for both rAAV2 and rAAV2i8 capsids (see Fig. S1a in the supplemental material). Similar to the transduction of rAAV2, cells transduced by rAAV2i8 in the INL were identified as rod bipolar cells and Müller glia (see Fig. S1b and c, arrowhead, in the supplemental

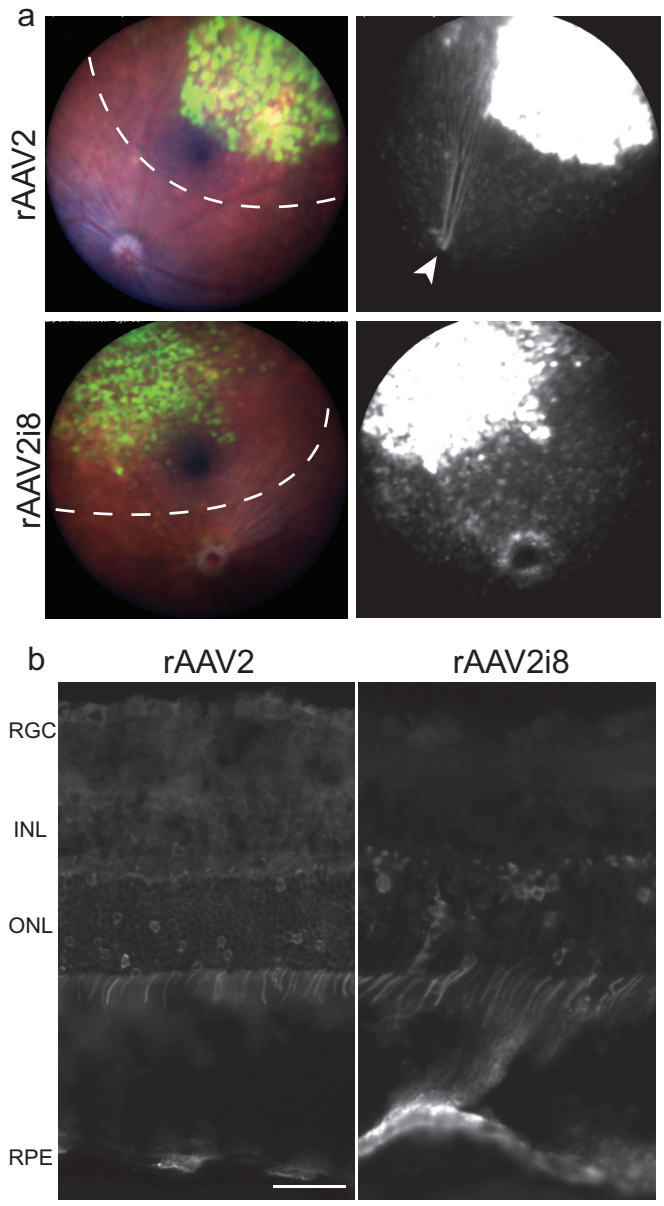

FIG 1 GFP fluorescence following subretinal delivery of rAAV2 and HS-deficient rAAV2i8 vector 8 weeks postinjection. (a) Representative fundus images and fluorescence of eyes treated with rAAV2i8 capsid and rAAV2 capsid. The dashed lines indicate detached areas of injection. Transduction was greatest in the bleb, but transduction of the RPE can be seen outside the initial bleb site. Transduction of ganglion cells can be observed by the GFP fluorescence of axons leading from the injection site to the optic disc in rAAV2-injected eyes (arrowhead). (b) Histology of eyes indicated similar transduction of RPE and ONL between rAAV2 and its HS-deficient rAAV2i8 vector. Expression of the INL and RGC by rAAV2 can be seen, but it is minimal for rAAV2i8. Scale bar = 20 μm.

material). These results confirm that the rAAV2i8 capsid is infectious in retinal tissue by SR delivery.

HS binding of rAAV2 is required for intravitreal transduction. Next, we were interested in assessing whether HS binding is necessary for IVit transduction of rAAV2. Both rAAV2 and rAAV2i8 capsids were delivered intravitreally to adult mice at a titer of 10^8 vg. rAAV2-injected eyes were fluorescent at the first imaging time point of 2 weeks, whereas rAAV2i8 showed no expression (data not shown). The eyes were evaluated for up to 12 weeks for the possibility of slower expression kinetics. During that time, rAAV2 fluorescence continued to increase, but no fluorescence was detected with rAAV2i8. By 12 weeks, rAAV2 capsid led to a diffuse pattern of fluorescence over the neural retina, as seen by fundus imaging (Fig. 2a). The rAAV2i8 capsid did not yield observable GFP fluorescence by fundoscopy, which resulted in a 300-fold reduction in GFP fluorescence (Fig. 2a). We tried a higher titer of 2×10^9 vg for both rAAV2 and its HS-binding mutant to maximize the chance to observe expression. Of course, the expression was much greater with higher titers of rAAV2 (see Fig. S2a in the supplemental material) than what was observed with the lower-titer-injected eyes (Fig. 2a), but the pattern of transduction remained unchanged. We confirmed that the vitreous did not specifically inhibit the transduction of the HS-ablated rAAV2i8 capsid. To do this, virus was mixed with vitreous and delivered subretinally. Both rAAV2 and rAAV2i8 shared intense expression throughout most of the retina observed on fundoscopy (see Fig. S3 in the supplemental material).

Eyes injected intravitreally with rAAV were further evaluated by IHC. rAAV2 transduction was mainly detected in the RGC and INL, and in some sections, transduction of photoreceptors could be observed (Fig. 2b, arrows). The histology of HS-ablated rAAV2 capsids revealed a dramatic lack of transduction, except for a few GFP-positive rods (Fig. 2b, arrows). Several mechanisms could be responsible for this phenotype. The lack of RGC and INL transduction with rAAV2i8 could be related to changes in either the tropism or te distribution of the capsid. We chose to further analyze the tissue using FISH to determine the distribution of transgenes following IVit delivery. This is a better alternative to IHC using antibodies against the capsid, since many of the capsid subunits would have dissociated to release the transgene. Similar to IHC expression, FISH signal for rAAV2-delivered transgenes was detected mainly in the RGC and INL (Fig. 2c). rAAV2i8-injected eyes showed transgenes were present in the ONL, but no signal was detected in either the RGC or the INL. These transgenes most likely represent episomes that are stable following entry into the retina by IVit delivery. It could be that the few transgenes in the ONL represent a subpopulation of retinal cells that form stable episomes, yet HS-deficient rAAV2 distributed similarly to rAAV2. Equally possible was the hypothesis that HS-ablated rAAV2 altered the distribution pattern within the retina.

HS binding is necessary for the vitreal accumulation of rAAV2 at the ILM in mice. To obtain a better understanding of the trafficking differences between the capsids following IVit delivery, eyes were enucleated soon after injection for FISH analysis. Because we had established that exposure of charged residues on the capsid surface plays an important role in transduction, we used FISH as an alternative to modifying the capsid with fluorescent particles for trafficking experiments. Previous reports had shown that AAV particles accumulate at the ILM 24 h postinjection (19), which was confirmed using our FISH protocol, indicating that we could detect transgenes carried in capsids that were still intact (data not shown). The time point was extended to 3 days postinjection to allow sufficient time for capsid accumulation at the ILM and to observe trafficking differences between the rAAV2 capsid and its HS-binding mutants. We used a range of doses to capture any concentration effect in accumulation and shortened the enzymatic time for FISH signal detection to give a more dy-

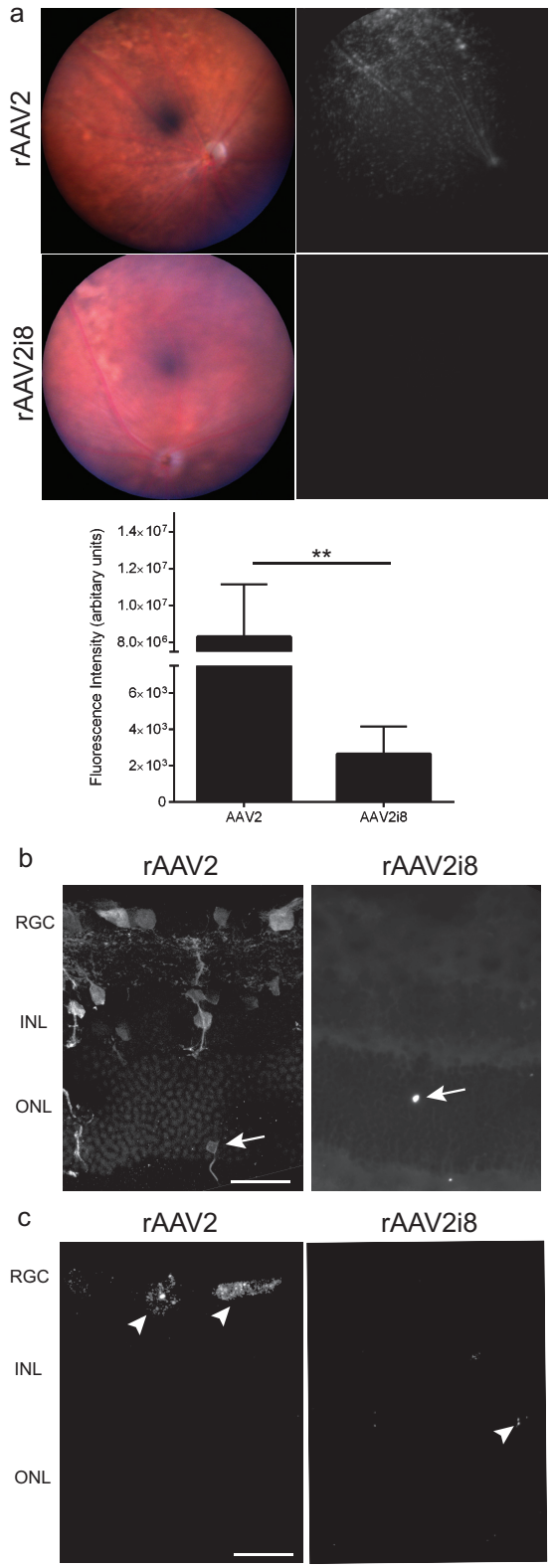

FIG 2 GFP fluorescence following intravitreal delivery of rAAV2 vector and its HS-binding-deficient variants 12 weeks postinjection. (a) (Top) Representative fundus images and fluorescence of eyes treated with rAAV2 capsid or rAAV2i8 capsid. rAAV2 capsid produced a large area of fluorescence, while the heparan sulfate-binding-deficient capsid showed no observable fluorescence. (Bottom) Quantification of fundus images showing a 300-fold decrease in expression between rAAV2 and rAAV2i8. The error bars indicate standard errors of the mean (SEM), and significance was detected by a nonparametric *t* test (**, $P < 0.01$). (b) IHC of rAAV2-injected retinas showing fluorescence mainly in the RGC, with fewer GFP-positive somas in the INL. rAAV2i8 showed minimal transduction of the retina. Rare transduction of photoreceptors could be observed (arrows). (c) FISH substrate was applied three times to maximize sensitivity and detected the locations of transgenes within the retina. Transgenes were detected mainly in the RGC and INL for rAAV2 capsid. A few GFP transgenes in the retina (arrowheads) were in the ONL for rAAV2i8. Scale bars = 20 μm.

namic range. PBS-injected eyes served as the negative control, which had minimal background labeling (Fig. 3a). With the shortened detection time, a dose of 1×10^8 vg had only weak signal in retinas for both rAAV2 and HS-deficient rAAV2-R585E capsids. At a dose of 5×10^8 vg, transgenes delivered by rAAV2 showed an accumulation at the ILM (Fig. 3a, arrows), as well as being present in the ONL (Fig. 3a, arrowheads). Without HS binding, rAAV2-R585E had only minimal signal in the ONL. At the highest dose tested (2×10^9 vg), rAAV2 resulted in even greater signal intensity at the ILM (Fig. 3a, arrows), showing increased accumulation of the vector. Additional aggregation of transgenes was seen in the ONL (Fig. 3a, arrowheads). At the same dose, a few rAAV2-R585E-delivered transgenes were detected in the ONL of the retina (Fig. 3a, arrowheads) but did not result in any accumulation at the ILM (Fig. 3a). Taken together, these results indicate (i) that HS binding on rAAV2 helps to accumulate vectors at the ILM, (ii) that this accumulation increases the number of transgenes residing in the retina, and (iii) that capsids can penetrate the retina from the vitreous without binding to HS, but to a far lesser extent (Fig. 3b). Once capsids pass through the ILM barrier, they seem capable of trafficking rapidly to distal layers of the outer retina. This highlights the fact that rAAV's rate-limiting step for efficient intravitreal transduction of the retina lies in the interaction between the capsid and the ILM.

HS binding is necessary for the vitreal accumulation of rAAV2 on human retinas. The abundant HSPG staining at the ILM in many animal models, including humans (see Fig. S4 in the supplemental material), suggests this mechanism may translate across species for human clinical applications. To evaluate this hypothesis, a viral binding assay was done on human retinas *ex vivo* by quartering the eye and leaving a small amount of vitreous attached to the retina to maintain the ILM structure. Vectors were applied to the vitreous, followed by harvesting of the various retinal layers. Transgenes carried by rAAV2 were bound to the retina, unlike those of the rAAV2i8 capsid (Fig. 4). The HS-deficient rAAV2i8 had relatively low vector binding in any of the collected tissues but did show a significant increase in binding to the choroid and sclera compared to rAAV2. Together with the mouse data, these results corroborate a mechanism in which HS binding promotes the accumulation of AAV vector out of the vitreous and onto the ILM for greater retinal penetration and transduction.

HS binding increases the IVit transduction of other rAAV serotypes. IVit transduction of other serotypes may benefit from the addition of the HS-binding motif and add to the diversity of vectors that could be used. The rAAV1 and rAAV6 serotypes differ by only 6 amino acids, with a single residue responsible for the difference in HSPG binding (39, 40). To evaluate the influence of HS binding between rAAV1 and rAAV6 retinal transduction for IVit transduction, the single-residue-mutant capsids were tested

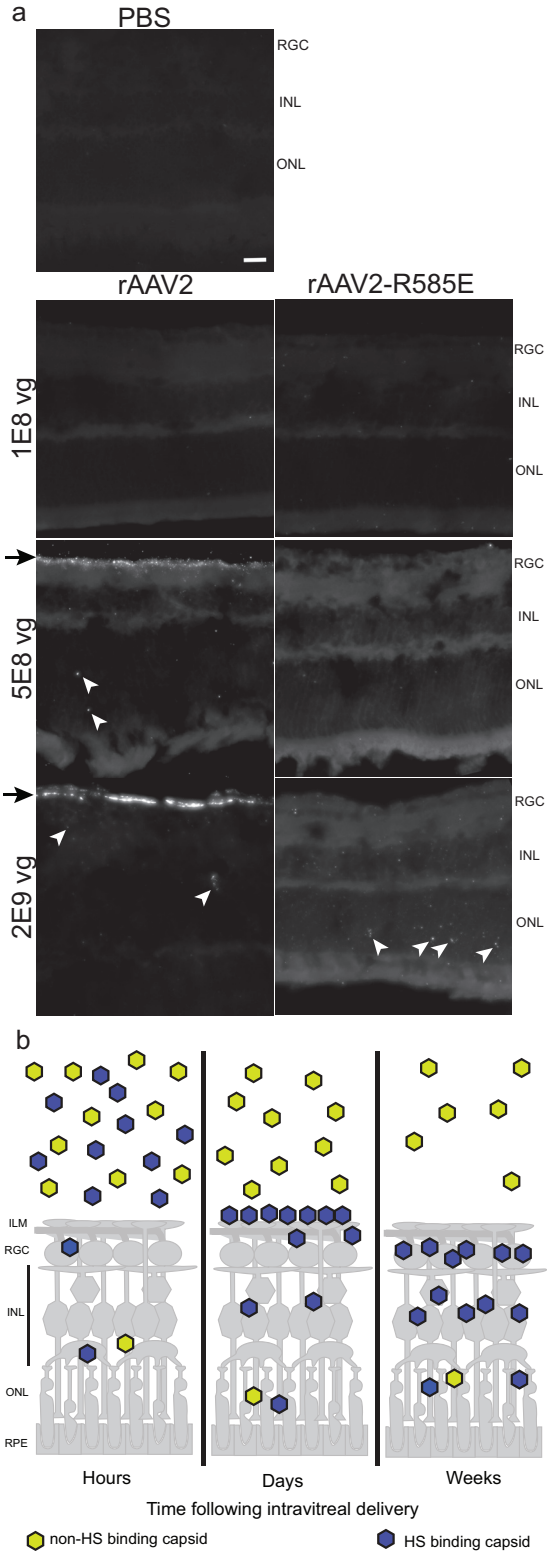

FIG 3 FISH of intravitreally injected eyes 3 days postinjection. (a) PBS-injected eyes served as a negative control for FISH detection and had low background. The arrowheads indicate FISH signal. Weak signal was detected in the retinas of eyes injected with 1×10^8 vg for rAAV2 and rAAV2-R585E. rAAV2 at a dose of 5×10^8vg showed accumulation of the transgene at the ILM (arrows), with some detectable transgenes in the outer retina (arrowheads). A dose of 5×10^8 vg led to weak signal for rAAV2-R585E. A high dose of 2×10^9 vg revealed greater accumulation of rAAV2 capsids at the ILM (arrows) and within the retina (arrowheads). At the same dose, rAAV2-R585E showed a greater presence in the retina within the ONL (arrowheads). (b) Schematic of the retina depicting the trafficking of rAAV following IVit delivery. Scale bar = 20 μm.

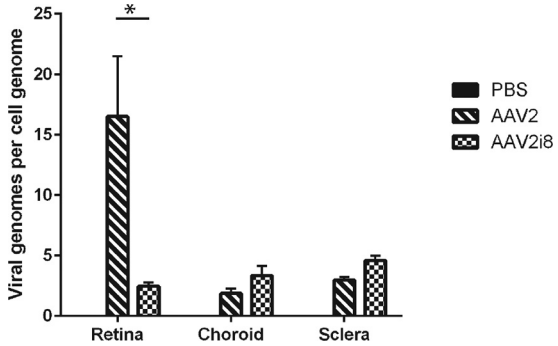

FIG 4 qPCR analysis of viral binding to human retinas *ex vivo*. The rAAV2 vector showed the greatest presence at the retina, with few transgenes found elsewhere. The numbers of transgenes delivered by rAAV2i8 were low in all collected tissues but showed a significant increase compared to rAAV2-delivered transgenes in both the choroid and sclera. The error bars indicate standard deviations. *, $P < 0.05$.

intravitreally in mice. Although rAAV1 and the HS-binding rAAV1-E531K had similar patterns of expression, rAAV1-E531K had 3-fold-greater GFP fluorescence than rAAV1 (Fig. 5a). The removal of HS binding in rAAV6 using the rAAV6-K531E capsid led to a reduction in retinal fluorescence by fundoscopy, as hypothesized (see Fig. S5a in the supplemental material). Both rAAV1 and rAAV6 capsids displayed a punctate expression pattern that clustered around the retinal vessels and that has been documented in other reports (23, 24). Because of the homology between rAAV1 and rAAV6, only rAAV1 and rAAV1-E531K were further evaluated for possible differences in cell tropism. IHC performed on these retinas showed the transduction of mainly Müller glia for both capsids by the colocalization of GFP and glutamine synthetase (Fig. 5b, arrowheads). Additional cells of the INL appeared to be transduced (Fig. 5b, arrows). In addition, both rAAV1 and rAAV1-E531K showed transduction of a few RGC and photoreceptors. The similar transduction patterns of rAAV1 and rAAV1-E531K indicate that HS binding had not altered the tropism of rAAV1. To confirm that the HS-binding mutation on rAAV1 does not convey use of HSPG for transduction, soluble heparin was mixed with capsids and applied to cells for an *in vitro* competition assay. rAAV2 required HSPG for *in vitro* transduction (4) and showed a dose-dependent decrease in transduction (see Fig. S6 in the supplemental material). Neither rAAV1 nor rAAV1-E531K transduction was affected at any heparin dose, indicating that the rAAV1-E531K capsid does not depend on HS binding for transduction. On average, transduction with rAAV1-E531K led to fewer GFP-positive cells than transduction with rAAV1, indicating that the single-amino-acid change alone does not provide an enhancement in transduction.

In the same article outlining the amino acid involved in rAAV1/rAAV6 transduction, a single-amino-acid mutant was identified on rAAV8, which provided HS-binding capability (39). Titers of rAAV8 and rAAV8-E533K were matched to 1×10^8 vg

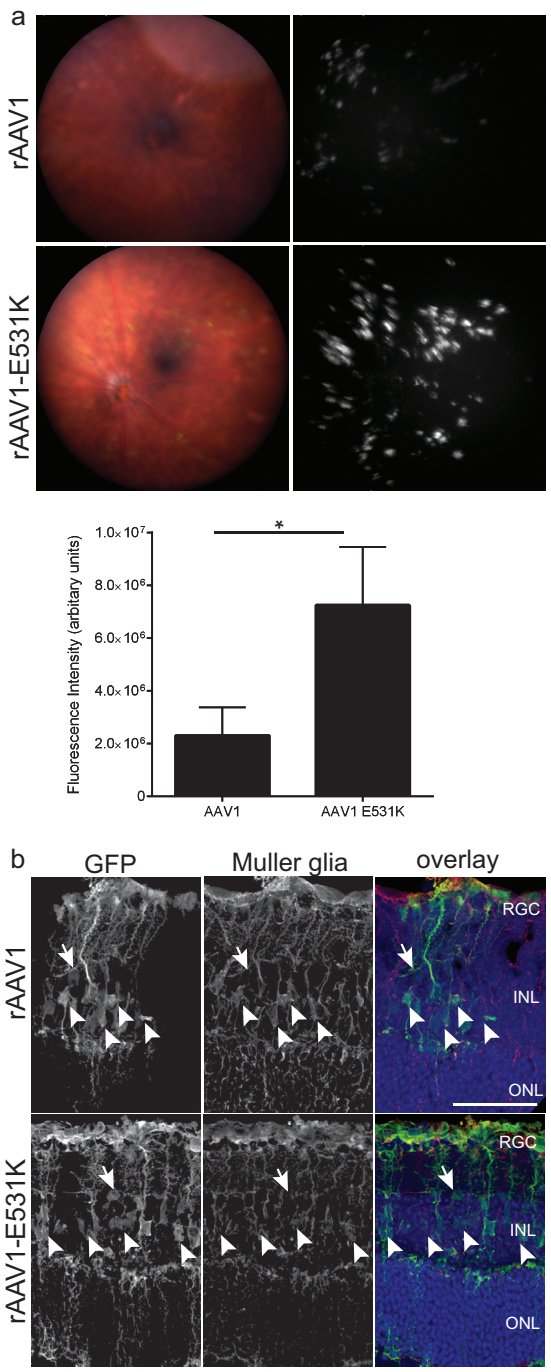

FIG 5 GFP fluorescence following intravitreal delivery of HS-binding variants of rAAV1 8 weeks postinjection. (a) (Top) Representative fundus images and fluorescence of eyes treated with rAAV1 capsid or rAAV1-E531K capsid. Both capsids produced punctate staining that clustered around the retinal vessels. (Bottom) Quantification of fundus images showing a 3-fold increase with rAAV1-E531K capsid compared to rAAV1 capsid. The error bars indicate SEM, and significance was determined by a nonparametric *t* test (*, $P < 0.05$). (b) GFP IHC of retinal sections 8 weeks after injection of rAAV1 and rAAV1-E531K capsids. The images show the colocalization (arrowheads) of GFP with Müller glia markers for rAAV1 and rAAV1-E531K. The individual channels show GFP and glutamine synthetase expression in the retina. Additional staining of non-Müller glia (arrows) can be seen. Confocal *z*-stack images were compressed and are displayed as maximum projections. Scale bar = 50 μm.

and injected intravitreally. At 8 weeks postadministration, fundus images revealed low GFP fluorescence for rAAV8 (see Fig. S7 in the supplemental material). Injection of eyes with rAAV8-E533K resulted in hazy fluorescence over the retina that, when quantified, was greater than that of the non-HS-binding parent serotype. We used FISH analysis to observe trafficking differences soon after injection and found again that HS binding promoted the accumulation of vector at the ILM and within the retina (see Fig. S8 in the supplemental material). These results suggest that HS binding alone is sufficient to enhance the transduction of intravitreally delivered AAV capsids by increasing the amount of vector that accumulates on the retina.

Other capsid motifs determine tropism over the HS-binding motif. The addition of the HS-binding motif helped to increase vector accumulation on the retina but did not alter the transduction pattern of rAAV1, indicating that native capsid motifs determine tropism. We were interested in determining if capsid motifs from other AAV serotypes could influence the transduction of rAAV2. A motif of rAAV1 was graphed onto the rAAV2 capsid using the rAAV2.5 capsid (41), which was delivered by IVit for analysis. While distinct from either parental serotype, the rAAV2.5 capsid revealed an expression pattern surrounding the retinal vessels (Fig. 6a). IHC of these eyes did not reveal any major tropism differences compared to rAAV2, in that RGC, Müller glia, and other cells of the INL were transduced by the chimeric capsid. A more recent paper has shown the amino acid at position 265 on the rAAV2.5 capsid to be solely responsible (42). Therefore, we tested an rAAV2-265D mutant capsid intravitreally, which revealed expression similar to that of the rAAV2.5 parent (see Fig. S9 in the supplemental material).

We chose to test an additional chimeric rAAV2 capsid that had dual HS and galactose binding capabilities. The chimeric rAAV2G9 was used and was found to have a punctate expression across the retina (Fig. 6b). The IHC showed a specific tropism to Müller glia. The galactose motif was structured from the rAAV9 capsid. By fundoscopy, both rAAV9 and HS-ablated rAAV2i8G9 capsids showed no expression following IVit delivery (see Fig. S10a in the supplemental material), indicating that galactose binding alone was insufficient to lead to transduction within the retina.

A double-chimeric capsid, rAAV2.5G9, was used to determine which of the capsid motifs, rAAV1 or rAAV9, was dominant. The intravitreal delivery of rAAV2.5G9 led to expression similar to that of the rAAV2.5 parent when imaged by fundoscopy (Fig. 6c). The fluorescence around the retinal vessels was very evident, with punctate expression found around the vessels. IHC of the rAAV2.5G9-injected eyes revealed a largely Müller glia-dominant tropism (Fig. 6c). Quantification of a comparison of all the fundoscopy expression showed rAAV2.5 and rAAV2.5G9 to have the highest transduction, with non-HS-binding capsids showing the lowest transduction (Fig. 6d). We used a lectin antibody to identify the presence of galactose throughout the retina; however, the majority of the staining occurred around the ONL without a clear connection to Müller glia (see Fig. S10b in the supplemental material). Therefore, the addition of either the rAAV1 or rAAV9 motif appeared to have equal abilities to control tropism, which is dominant over the tropism provided by the HS-binding motif.

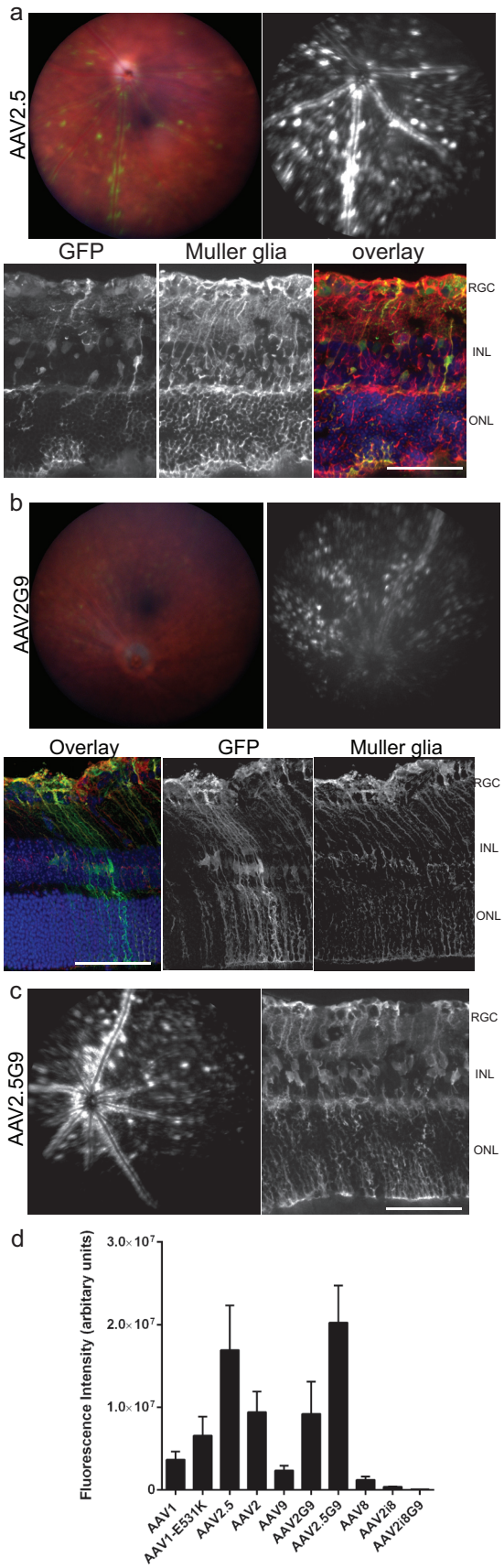

DISCUSSION

With the experiments conducted in this study, we gained a greater understanding of the early trafficking of rAAV following intravitreal delivery. As virus is injected into the vitreous, it radiates outward from the needle and travels through the vitreous humor. This stochastic dispersion of vector in the vitreous results in a dilution of the vector concentration. Once at the junction, the capsid interacts with the glycans present on the ILM to effectively concentrate the virus outside the vitreous. This interaction occurs on the order of days following delivery. After concentration of the virus, the vector begins to penetrate the retinal layers, where it infects various retinal cells. In the weeks after delivery, transgene expression is detectable and remains so for months. Not all AAV serotypes aggregate sufficiently to promote penetration into the retina and to lead to transgene expression. This can be circumvented through the application of HS-binding motifs on the capsid, thereby allowing the capsid to interact with the ILM without causing a change in tropism.

The interaction of rAAV capsids with the ILM is the rate-limiting step for retinal trafficking (19, 20). Therefore, interaction with the membrane should be increased to maximize the number of capsids entering the retina. Pores present in the ILM may explain why few HS-binding-deficient capsids were able to pass through the ILM and traffic rapidly to the outer retina (Fig. 3; see Fig. S8 in the supplemental material). Similar numbers of rAAV2 capsids were found rapidly in the outer retina, supporting the idea of a non-glycan-mediated entry, as through a pore. These deeply penetrating vectors may represent the few capsids whose trajectories were aligned to allow them to quickly pass through the pores and through the retinal interior. However, the majority of vectors must interact with the ILM before they can penetrate into the retina. If capsids cannot interact with the ILM, they remain diluted in the vitreous, unable to transduce the retina. Even if a higher concentration of vector is used, the lack of interaction with the ILM prevents capsids from aggregating onto the retina surface and transducing the retina. We were able to increase the amount of vector in the retina by adding an HS-binding motif to the non-HS-binding capsids. Currently, the methods for getting vector into the retina using high-titer virus are to either digest the ILM or perform a sub-ILM injection (19–21, 43). It is easy to see how development of better capsids that are capable of transducing without these aids would be of interest to researchers and clinicians alike.

The ILM structure is found across multiple species (see Fig. S4 in the supplemental material) and could serve to attract and concentrate rAAV capsids outside the vitreous, not just for mice, but also for humans. As hypothesized, we found the same accumula-

FIG 6 Chimeric capsids suggest tropism is influenced by motifs other than HS binding. (a) Elements of rAAV1 were applied to rAAV2 using the chimeric rAAV2.5 capsid and imaged for intravitreal delivery. The histology of rAAV2.5 showed transduction of Müller glia, as seen with glutamine synthetase colabeling. In addition, RGC expression is present. (b) Elements of rAAV9 were applied to rAAV2 using the chimeric rAAV2G9. Histology of rAAV2G9 showed mostly transduction of Müller glia, as seen with glutamine synthetase colabeling. (c) Transduction of the double-chimera rAAV2.5G9 capsid showed a transduction profile similar to that of the rAAV2.5 parent capsid, as seen by fundus imaging, and showed Müller glial transduction by IHC. (d) Quantification of the fundus fluorescence for the collection of capsids. The error bars represent SEM. Scale bars = 50 μm.

tion on the retina with only the HS-binding rAAV2 using human *ex vivo* retinas (Fig. 4). The kinetics of vector dispersion through the vitreous humor are likely to be slower due to the volume, which also means longer times until interaction with the ILM and penetration into the retina. Studies in nonhuman primates revealed that vector accumulated at the ILM 1 month after intravitreal injection but remained abundant in the vitreous (data not shown). Although these kinetic studies must be worked out further for primate intravitreal delivery, the mechanism by which HS-binding motifs positively influence vector accumulation on the retina will make vectors more effective. It is important to remember that the transduction observed in a mouse model may not be relevant to other models. While the mouse has become a standard model for retinal gene transfer, certain size and anatomical differences exist between them and larger-animal models. In addition, the thickness differences of the ILM between mice and primates may lead to selection of capsids that are not as efficient across species. However, through the addition of the HS-binding motif, we showed that our mechanism of vector accumulation is conserved in both mouse and primate retinas.

The interaction between the AAV capsid and HS is mediated by a static charge. The negative charge of the sulfate groups on the heparan chain, which are found on the proteoglycan core of HSPG, serves to attract the basic patch of residues on the rAAV2 capsid. Through this sulfate interaction, the heparin chain falls along the inner surface of the 3-fold protrusion of the capsid surface. We used capsid mutants to change this charge interaction to no longer attract the sulfate group and to obstruct the heparan chain interaction with the capsid. It could be argued that this charge interaction is the most important interaction between rAAV and the ILM; therefore, the capsid is really drawn to any highly charged molecule. We used dextran sulfate to act as a surrogate for heparan sulfate. We mixed rAAV2 capsids with dextran sulfate or heparan sulfate (heparin) or unsulfated heparan sulfate (heparosan) before IVit delivery. We found that heparin and heparosan dramatically decreased transduction of rAAV2, while dextran sulfate resulted in no change (data not shown). These data indicate that rAAV2 specifically interacts with HSPG, not through electrostatic charge alone. Therefore, random changes to make the capsid more charged may have little influence.

Indeed, HS binding led to greater presence of transgenes in the retina than the parent capsid when assessed by FISH soon after injection (Fig. 3). Transgenes of non-HS-binding rAAV1 and rAAV8 could still be detected in the retina, but to a lesser extent (see Fig. S8 in the supplemental material). The lack of expression with HS-binding rAAV3 when injected intravitreally (data not shown) was expected, because the serotype is inefficient in the transduction of most cell types (44) and may encounter additional barriers to efficient transduction of cells. rAAV6 is a serotype of interest for retinal transduction and has been modified to increase the specific transduction of Müller glia using the ShH10 capsid (45). Without HS binding, the ShH10 vector may show much weaker fluorescence. Based on our data, we suggest that any capsid that has an HS-binding motif would be capable of accumulating at the ILM. The recent study published by Boye et al. used HSPG-binding rAAV5 and rAAV8 but was unsuccessful in enhancing their GFP fluorescence, indicating this HS-binding enhancement is not universal to all capsids (46). We believe this to be related to their shortened CBA promoter and that use of a different promoter may reveal expression. We showed that HSPG binding on rAAV8-CBh-GFP is capable of enhancing accumulation and expression. As predicted by our model and validated by FISH, this was due to the HSPG binding-mediated interaction with the ILM. We predict that rAAV5 capsid should have enhanced transduction with the HSPG-binding mutation. In addition, other laboratories have tested rAAV5 and rAAV8 using a CAG promoter and have shown expression (47). This serves as a reason to reevaluate all rAAV capsid transduction following intravitreal delivery by FISH. Using GFP expression as the only way to analyze where capsids have trafficked in the retina provides an incomplete picture of how rAAV traffics in the retina following IVit delivery. FISH analysis provides a simple way to detect the locations of viral transgenes as a surrogate for the locations of capsids. This provides a better alternative to modifying the capsid surface with fluorescent Cy3 dye, which binds to the Lys residues on the capsid. Modifying the rAAV1 capsid to have more Lys residues (rAAV1-E531K), which then bind to HSPG, increases transduction, so it could be argued that the Cy3 dye could have masked the expression of serotypes in earlier studies (19, 20).

Increasing the virus concentration could increase vector interaction with ILM but is more likely to evoke an immune response, as the vitreal space is not immune privileged like the subretinal space (48). Therefore, it is optimal to use lower concentrations of vector to avoid this response. This is why we chose to work with a low concentration of vector to maximize expression rather than using high titers of vector. Other laboratories sought to maximize expression in other ways. In a recent study, selection of a peptide incorporated into the rAAV2 capsid showed ONL transduction from the vitreous in both mice and nonhuman primates (49). While this peptide is located near the HS-binding footprint, the capsid shows a dependency on HSPG for transduction and may still exploit the same HS-mediated accumulation mechanism outlined here. We tested this hypothesis by using the amino acid mutants discussed here, along with the peptide, delivered intravitreally to adult mice. As predicted by our model, GFP expression was detected only when the Arg residues involved in the HS-binding motif were present (data not shown). We found that the peptide insertion reduced rAAV2 transduction, suggesting that a reduction in HSPG binding is met with a reduction in IVit transduction. A recent publication has reported that the mechanism exploited by the peptide is intracellular (47). Other attempts to enhance transduction used capsids modified to avoid proteasomal degradation (50), thereby enhancing intracellular trafficking to help increase the transgene expression of intravitreally delivered capsids. However, a recent publication suggests that these vectors may not benefit from proteasome avoidance (46). These capsid changes work downstream of ILM binding once the vector has penetrated the retina. To take advantage of the retinal structure, binding to the ILM can be used to accumulate vectors at the retina for transduction. This is likely why rAAV2 has been successful at intravitreal retinal transduction.

Although HSPG is abundant at the ILM, other receptors can play a role in the transduction of the retina from the vitreous. The transduction by rAAV1 and rAAV6 suggests the presence of 2,3- or 2,6-N-linked sialic acid at the ILM despite the lack of staining in that region (data not shown). The pattern of transduction observed by fundus imaging may indicate a distinct pattern of this sialic acid in the retina that is not visible by histology but that could be seen by flat-mount staining. It would be beneficial to perform FISH on whole-mount retinas soon after injection to

observe accumulation of vector. It may be that these serotypes aggregate only at specific retinal structures or that vector aggregates along the entire inner retinal surface but leads to transduction only in specific regions. By performing FISH on whole mounts, we would gain a better understanding of the phenotype observed with the chimeric rAAV2.5 and rAAV2G9 capsids. Other forms of sialic acid known to interact with rAAV4 and rAAV5 may not be expressed abundantly at the ILM or could be masked by other glycans. This would explain the lack of transduction by these serotypes when compared in a normal mouse retina. In addition to sialic acid, laminin staining is abundant at the ILM and is restricted to the blood vessels. Laminin receptor is known to interact with the rAAV2, rAAV3, rAAV8, and rAAV9 serotypes (10). Although these capsids can interact with laminin receptors at the vitreoretinal junction, this interaction seems insufficient to promote efficient intravitreal retinal transduction. Again, a reevaluation of all rAAV serotypes using FISH as the detection method would provide a greater understanding of virus trafficking and transduction in the retina.

The similar transduction profiles of SR-delivered rAAV2 and rAAV2i8 indicate that rAAV2 does not require HS binding for retinal transduction (Fig. 1). It may be that subretinal delivery effectively concentrates the vector, thereby stoichiometrically skewing capsids toward expression. In addition to transduction by receptor-mediated endocytosis, SR delivery provides abundant rAAV vectors to the phagocytic RPE and may explain why the RPE appears to be the primary cell target of both rAAV2 and rAAV2i8. Regardless of affinity for any particular cell type, rAAV2 and rAAV2i8 vectors lead to transduction of RPE, rods, cones, rod bipolar cells, and Müller glia (see Fig. S1 in the supplemental material). The majority of these transduced cells are located within the injection bleb, but transduction of the RPE can be seen far outside the detached area. It would be of interest to see if the RGC transduction of subretinally delivered rAAV2 is due to the HSPG on the ILM pulling on the vector. FISH could be used to map the trafficking of SR-delivered vector to better understand this phenomenon.

ACKNOWLEDGMENTS

We are grateful for the human tissue provided by donors and Miracles in Sight. We extend our appreciation to Thomas B. Lentz, Matthew L. Hirsch, Eric L. Hastie, Chengwen Li, and Aravind Asokan for their assistance in the production and editing of the manuscript. We are grateful for the advice and insight provided by Peter A. Campochiaro and Jean Bennett. The Histology Research Core Facility in the Department of Cell Biology and Physiology at the University of North Carolina (UNC), Chapel Hill, NC, provided some of the histology slides.

R. Jude Samulski is the founder and a shareholder at Asklepios BioPharmaceutical. He receives research support through UNC from Asklepios BioPharmaceutical. He holds patents that have been licensed by UNC to Asklepios Biopharmaceutical, for which he receives royalties. He has consulted for Baxter Healthcare and has received payment for speaking.

FUNDING INFORMATION

This work, including the efforts of R. Jude Samulski, was funded by HHS | National Institutes of Health (NIH) (5103757). This work, including the efforts of Kenton T. Woodard, was funded by Howard Hughes Medical Institute (HHMI) (Translational Medicine Program).

Center funds were used for this paper.

REFERENCES

1. **Daya S, Berns KI.** 2008. Gene therapy using adeno-associated virus vectors. Clin Microbiol Rev **21:**583–593. http://dx.doi.org/10.1128/CMR.00008-08.
2. **Hastie E, Samulski RJ.** 2015. Adeno-associated virus at 50: a golden anniversary of discovery, research, and gene therapy success; a personal perspective. Hum Gene Ther **26:**257–265. http://dx.doi.org/10.1089/hum.2015.025.
3. **Mitchell AM, Nicolson SC, Warischalk JK, Samulski RJ.** 2010. AAV's anatomy: roadmap for optimizing vectors for translational success. Curr Gene Ther **10:**319–340. http://dx.doi.org/10.2174/156652310793180706.
4. **Summerford C, Samulski RJ.** 1998. Membrane-associated heparan sulfate proteoglycan is a receptor for adeno-associated virus type 2 virions. J Virol **72:**1438–1445.
5. **Wu Z, Miller E, Agbandje-McKenna M, Samulski RJ.** 2006. Alpha2,3 and alpha2,6 N-linked sialic acids facilitate efficient binding and transduction by adeno-associated virus types 1 and 6. J Virol **80:**9093–9103. http://dx.doi.org/10.1128/JVI.00895-06.
6. **Wu Z, Asokan A, Samulski RJ.** 2006. Adeno-associated virus serotypes: vector toolkit for human gene therapy. Mol Ther **14:**316–327. http://dx.doi.org/10.1016/j.ymthe.2006.05.009.
7. **Kaludov N, Brown KE, Walters RW, Zabner J, Chiorini JA.** 2001. Adeno-associated virus serotype 4 (AAV4) and AAV5 both require sialic acid binding for hemagglutination and efficient transduction but differ in sialic acid linkage specificity. J Virol **75:**6884–6893. http://dx.doi.org/10.1128/JVI.75.15.6884-6893.2001.
8. **Shen S, Bryant KD, Brown SM, Randell SH, Asokan A.** 2011. Terminal N-linked galactose is the primary receptor for adeno-associated virus 9. J Biol Chem **286:**13532–13540. http://dx.doi.org/10.1074/jbc.M110.210922.
9. **Qing K, Mah C, Hansen J, Zhou S, Dwarki V, Srivastava A.** 1999. Human fibroblast growth factor receptor 1 is a co-receptor for infection by adeno-associated virus 2. Nat Med **5:**71–77. http://dx.doi.org/10.1038/4758.
10. **Akache B, Grimm D, Pandey K, Yant SR, Xu H, Kay MA.** 2006. The 37/67-kilodalton laminin receptor is a receptor for adeno-associated virus serotypes 8, 2, 3, and 9. J Virol **80:**9831–9836. http://dx.doi.org/10.1128/JVI.00878-06.
11. **Summerford C, Bartlett JS, Samulski RJ.** 1999. AlphaVbeta5 integrin: a co-receptor for adeno-associated virus type 2 infection. Nat Med **5:**78–82. http://dx.doi.org/10.1038/4768.
12. **Hauswirth WW.** 2014. Retinal gene therapy using adeno-associated viral vectors: multiple applications for a small virus. Hum Gene Ther **25:**671–678. http://dx.doi.org/10.1089/hum.2014.2530.
13. **Maguire AM, Simonelli F, Pierce EA, Pugh EN, Mingozzi F, Bennicelli J, Banfi S, Marshall KA, Testa F, Surace EM, Rossi S, Lyubarsky A, Arruda VR, Konkle B, Stone E, Sun J, Jacobs J, Dell'Osso L, Hertle R, Ma J-X, Redmond TM, Zhu X, Hauck B, Zelenaia O, Shindler KS, Maguire MG, Wright JF, Volpe NJ, McDonnell JW, Auricchio A, High KA, Bennett J.** 2008. Safety and efficacy of gene transfer for Leber's congenital amaurosis. N Engl J Med **358:**2240–2248. http://dx.doi.org/10.1056/NEJMoa0802315.
14. **Hauswirth WW, Aleman TS, Kaushal S, Cideciyan AV, Schwartz SB, Wang L, Conlon TJ, Boye SL, Flotte TR, Byrne BJ, Jacobson SG.** 2008. Treatment of leber congenital amaurosis due to RPE65 mutations by ocular subretinal injection of adeno-associated virus gene vector: short-term results of a phase I trial. Hum Gene Ther **19:**979–990. http://dx.doi.org/10.1089/hum.2008.107.
15. **Boye SE, Boye SL, Lewin AS, Hauswirth WW.** 2013. A comprehensive review of retinal gene therapy. Mol Ther **21:**509–519. http://dx.doi.org/10.1038/mt.2012.280.
16. **Trapani I, Puppo A, Auricchio A.** 2014. Vector platforms for gene therapy of inherited retinopathies. Prog Retin Eye Res **43:**108–128. http://dx.doi.org/10.1016/j.preteyeres.2014.08.001.
17. **Natkunarajah M, Trittibach P, McIntosh J, Duran Y, Barker SE, Smith AJ, Nathwani AC, Ali RR.** 2008. Assessment of ocular transduction using single-stranded and self-complementary recombinant adeno-associated virus serotype 2/8. Gene Ther **15:**463–467. http://dx.doi.org/10.1038/sj.gt.3303074.
18. **Allocca M, Mussolino C, Garcia-Hoyos M, Sanges D, Iodice C, Petrillo M, Vandenberghe LH, Wilson JM, Marigo V, Surace EM, Auricchio A.** 2007. Novel adeno-associated virus serotypes efficiently transduce murine

photoreceptors. J Virol **81:**11372–11380. http://dx.doi.org/10.1128/JVI.01327-07.
19. **Dalkara D, Kolstad KD, Caporale N, Visel M, Klimczak RR, Schaffer DV, Flannery JG.** 2009. Inner limiting membrane barriers to AAV-mediated retinal transduction from the vitreous. Mol Ther **17:**2096–2102. http://dx.doi.org/10.1038/mt.2009.181.
20. **Kolstad KD, Dalkara D, Guerin K, Visel M, Hoffmann N, Schaffer DV, Flannery JG.** 2010. Changes in adeno-associated virus-mediated gene delivery in retinal degeneration. Hum Gene Ther **21:**571–578. http://dx.doi.org/10.1089/hum.2009.194.
21. **Yin L, Greenberg K, Hunter JJ, Dalkara D, Kolstad KD, Masella BD, Wolfe R, Visel M, Stone D, Libby RT, Diloreto D, Schaffer D, Flannery J, Williams DR, Merigan WH.** 2011. Intravitreal injection of AAV2 transduces macaque inner retina. Invest Ophthalmol Vis Sci **52:**2775–2783. http://dx.doi.org/10.1167/iovs.10-6250.
22. **Ivanova E, Hwang G-S, Pan Z-H, Troilo D.** 2010. Evaluation of AAV-mediated expression of Chop2-GFP in the marmoset retina. Invest Ophthalmol Vis Sci **51:**5288–5296. http://dx.doi.org/10.1167/iovs.10-5389.
23. **Pellissier LP, Hoek RM, Vos RM, Aartsen WM, Klimczak RR, Hoyng SA, Flannery JG, Wijnholds J.** 2014. Specific tools for targeting and expression in Müller glial cells. Mol Ther Methods Clin Dev **1:**14009. http://dx.doi.org/10.1038/mtm.2014.9.
24. **Aartsen WM, van Cleef KWR, Pellissier LP, Hoek RM, Vos RM, Blits B, Ehlert EME, Balaggan KS, Ali RR, Verhaagen J, Wijnholds J.** 2010. GFAP-driven GFP expression in activated mouse Müller glial cells aligning retinal blood vessels following intravitreal injection of AAV2/6 vectors. PLoS One **5:**e12387. http://dx.doi.org/10.1371/journal.pone.0012387.
25. **Hellström M, Ruitenberg MJ, Pollett MA, Ehlert EME, Twisk J, Verhaagen J, Harvey AR.** 2009. Cellular tropism and transduction properties of seven adeno-associated viral vector serotypes in adult retina after intravitreal injection. Gene Ther **16:**521–532. http://dx.doi.org/10.1038/gt.2008.178.
26. **Halfter W, Dong S, Dong A, Eller AW, Nischt R.** 2008. Origin and turnover of ECM proteins from the inner limiting membrane and vitreous body. Eye **22:**1207–1213. http://dx.doi.org/10.1038/eye.2008.19.
27. **Candiello J, Balasubramani M, Schreiber EM, Cole GJ, Mayer U, Halfter W, Lin H.** 2007. Biomechanical properties of native basement membranes. FEBS J **274:**2897–2908. http://dx.doi.org/10.1111/j.1742-4658.2007.05823.x.
28. **Cehajic-Kapetanovic J, Le Goff MM, Allen A, Lucas RJ, Bishop PN.** 2011. Glycosidic enzymes enhance retinal transduction following intravitreal delivery of AAV2. Mol Vis **17:**1771–1783.
29. **Asokan A, Conway JC, Phillips JL, Li C, Hegge J, Sinnott R, Yadav S, DiPrimio N, Nam H-J, Agbandje-McKenna M, McPhee S, Wolff J, Samulski RJ.** 2010. Reengineering a receptor footprint of adeno-associated virus enables selective and systemic gene transfer to muscle. Nat Biotechnol **28:**79–82. http://dx.doi.org/10.1038/nbt.1599.
30. **Kern A, Schmidt K, Leder C, Müller OJ, Wobus CE, Bettinger K, Von der Lieth CW, King JA, Kleinschmidt JA.** 2003. Identification of a heparin-binding motif on adeno-associated virus type 2 capsids. J Virol **77:**11072–11081. http://dx.doi.org/10.1128/JVI.77.20.11072-11081.2003.
31. **Gray SJ, Nagabhushan Kalburgi S, McCown TJ, Jude Samulski R.** 2013. Global CNS gene delivery and evasion of anti-AAV-neutralizing antibodies by intrathecal AAV administration in non-human primates. Gene Ther **20:**450–459. http://dx.doi.org/10.1038/gt.2012.101.
32. **Yokoi K, Kachi S, Zhang HS, Gregory PD, Spratt SK, Samulski RJ, Campochiaro PA.** 2007. Ocular gene transfer with self-complementary AAV vectors. Invest Ophthalmol Vis Sci **48:**3324–3328. http://dx.doi.org/10.1167/iovs.06-1306.
33. **Kong F, Li W, Li X, Zheng Q, Dai X, Zhou X, Boye SL, Hauswirth WW, Qu J, Pang J-J.** 2010. Self-complementary AAV5 vector facilitates quicker transgene expression in photoreceptor and retinal pigment epithelial cells of normal mouse. Exp Eye Res **90:**546–554. http://dx.doi.org/10.1016/j.exer.2010.01.011.
34. **Gray SJ, Foti SB, Schwartz JW, Bachaboina L, Taylor-Blake B, Coleman J, Ehlers MD, Zylka MJ, McCown TJ, Samulski RJ.** 2011. Optimizing promoters for recombinant adeno-associated virus-mediated gene expression in the peripheral and central nervous system using self-complementary vectors. Hum Gene Ther **22:**1143–1153. http://dx.doi.org/10.1089/hum.2010.245.
35. **Grieger JC, Choi VW, Samulski RJ.** 2006. Production and characterization of adeno-associated viral vectors. Nat Protoc **1:**1412–1428. http://dx.doi.org/10.1038/nprot.2006.207.
36. **Shen S, Horowitz ED, Troupes AN, Brown SM, Pulicherla N, Samulski RJ, Agbandje-McKenna M, Asokan A.** 2013. Engraftment of a galactose receptor footprint onto adeno-associated viral capsids improves transduction efficiency. J Biol Chem **288:**28814–28823. http://dx.doi.org/10.1074/jbc.M113.482380.
37. **Giove TJ, Sena-Esteves M, Eldred WD.** 2010. Transduction of the inner mouse retina using AAVrh8 and AAVrh10 via intravitreal injection. Exp Eye Res **91:**652–659. http://dx.doi.org/10.1016/j.exer.2010.08.011.
38. **Ogata N, Matsushima M, Takada Y, Tobe T, Takahashi K, Yi X, Yamamoto C, Yamada H, Uyama M.** 1996. Expression of basic fibroblast growth factor mRNA in developing choroidal neovascularization. Curr Eye Res **15:**1008–1018. http://dx.doi.org/10.3109/02713689609017649.
39. **Wu Z, Asokan A, Grieger JC, Govindasamy L, Agbandje-McKenna M, Samulski RJ.** 2006. Single amino acid changes can influence titer, heparin binding, and tissue tropism in different adeno-associated virus serotypes. J Virol **80:**11393–11397. http://dx.doi.org/10.1128/JVI.01288-06.
40. **Arnett ALH, Beutler LR, Quintana A, Allen J, Finn E, Palmiter RD, Chamberlain JS.** 2013. Heparin-binding correlates with increased efficiency of AAV1- and AAV6-mediated transduction of striated muscle, but negatively impacts CNS transduction. Gene Ther **20:**497–503. http://dx.doi.org/10.1038/gt.2012.60.
41. **Bowles DE, McPhee SW, Li C, Gray SJ, Samulski JJ, Camp AS, Li J, Wang B, Monahan PE, Rabinowitz JE, Grieger JC, Govindasamy L, Agbandje-McKenna M, Xiao X, Samulski RJ.** 2012. Phase 1 gene therapy for Duchenne muscular dystrophy using a translational optimized AAV vector. Mol Ther **20:**443–455. http://dx.doi.org/10.1038/mt.2011.237.
42. **Li C, Diprimio N, Bowles DE, Hirsch ML, Monahan PE, Asokan A, Rabinowitz J, Agbandje-McKenna M, Samulski RJ.** 2012. Single amino acid modification of adeno-associated virus capsid changes transduction and humoral immune profiles. J Virol **86:**7752–7759. http://dx.doi.org/10.1128/JVI.00675-12.
43. **Boye SE, Alexander JJ, Witherspoon CD, Boye SL, Peterson JJ, Clark M, Sandefer KJ, Girkin CA, Hauswirth WW, Gamlin PD.** 2016. Highly efficient delivery of AAV vectors to the primate retina. Hum Gene Ther **27:**580–597. http://dx.doi.org/10.1089/hum.2016.085.
44. **Messina EL, Nienaber J, Daneshmand M, Villamizar N, Samulski J, Milano C, Bowles DE.** 2012. Adeno-associated viral vectors based on serotype 3b use components of the fibroblast growth factor receptor signaling complex for efficient transduction. Hum Gene Ther **23:**1031–1042. http://dx.doi.org/10.1089/hum.2012.066.
45. **Klimczak RR, Koerber JT, Dalkara D, Flannery JG, Schaffer DV.** 2009. A novel adeno-associated viral variant for efficient and selective intravitreal transduction of rat Müller cells. PLoS One **4:**e7467. http://dx.doi.org/10.1371/journal.pone.0007467.
46. **Boye SL, Bennett A, Scalabrino ML, McCullough KT, Van Vliet K, Choudhury S, Ruan Q, Peterson J, Agbandje-McKenna M, Boye SE.** 2016. Impact of heparan sulfate binding on transduction of retina by recombinant adeno-associated virus vectors. J Virol **90:**4215–4231. http://dx.doi.org/10.1128/JVI.00200-16.
47. **Khabou H, Desrosiers M, Winckler C, Fouquet S, Auregan G, Bemelmans AP, Sahel JA, Dalkara D.** 4 June 2016. Insight into the mechanisms of enhanced retinal transduction by the engineered AAV2 capsid variant -7m8. Biotechnol Bioeng. http://dx.doi.org/10.1002/bit.26031.
48. **Li Q, Miller R, Han P-Y, Pang J, Dinculescu A, Chiodo V, Hauswirth WW.** 2008. Intraocular route of AAV2 vector administration defines humoral immune response and therapeutic potential. Mol Vis **14:**1760–1769.
49. **Kay CN, Ryals RC, Aslanidi GV, Min SH, Ruan Q, Sun J, Dyka FM, Kasuga D, Ayala AE, Van Vliet K, Agbandje-McKenna M, Hauswirth WW, Boye SL, Boye SE.** 2013. Targeting photoreceptors via intravitreal delivery using novel, capsid-mutated AAV vectors. PLoS One **8:**e62097. http://dx.doi.org/10.1371/journal.pone.0062097.
50. **Petrs-Silva H, Dinculescu A, Li Q, Min S-H, Chiodo V, Pang J-J, Zhong L, Zolotukhin S, Srivastava A, Lewin AS, Hauswirth WW.** 2009. High-efficiency transduction of the mouse retina by tyrosine-mutant AAV serotype vectors. Mol Ther **17:**463–471. http://dx.doi.org/10.1038/mt.2008.269.